

## Full Paper

# Use of Nanodiamonds as a Reducing Agent in a Chlorate-based Energetic Composition

Marc Comet\*, Vincent Pichot, Benny Siegert, Denis Spitzer

NS3E Nanomatériaux pour les Systèmes Sous Sollicitations Extrêmes, UMR CNRS-ISL no 320, Institut Franco-Allemand de Recherches de Saint-Louis (ISL), 5 Rue du Général Cassagnou, P.O.B. 70034, 68301 Saint-Louis Cedex (France)

Jean-Pierre Moeglin

OAL Optronique, Applications des Lasers, Institut Franco-Allemand de Recherches de Saint-Louis (ISL), 5 Rue du Général Cassagnou, P.O.B. 70034, 68301 Saint-Louis Cedex (France)

Yannick Boehrer

VP Vidéo, Photo, Institut Franco-Allemand de Recherches de Saint-Louis (ISL), 5 Rue du Général Cassagnou, P.O.B. 70034, 68301 Saint-Louis Cedex (France)

Received: February 13, 2007

DOI: 10.1002/prop.200700900

## Abstract

To our knowledge, the incorporation of nanodiamond (nD) as a reducing agent in an energetic composition has never been reported in the literature. Diamond exhibits particularly interesting physico-chemical properties: high density, good energetic potential, and relatively low thermal sensitivity. This study proposes to demonstrate that an explosive energetic composition can be obtained by physical mixing of nD and potassium chlorate (PC). First, the energetic characteristics of this formulation were compared to those of the famous “white powder” made of PC and saccharose and discovered by the French chemist Berthollet in the 18th century. In the second part, the combustion of pelletized nD-based mixtures initiated by a laser beam was studied by time resolved cinematography. The deflagration velocity was measured on the most energetic composition, which has a slightly negative oxygen balance ( $OB = -30.1\%$ ).

**Keywords:** Chlorate, Energetic Composition, Nanodiamond

## 1 Introduction

The goal of this study was to demonstrate that diamond structured at the nanoscale can be used as an efficient reducing agent in an energetic explosive composition. For this purpose, the nanodiamonds (nDs) were mixed with potassium chlorate (PC), which is not an intrinsic explosive [1]. Thus, the observed explosive properties result from the interaction between this compound and nD. This work proposes to determine the

influence of diamond on the characteristics and the energetic performance of an nD/PC mixture.

The explosive properties of chlorate-based energetic compositions were observed by Berthollet [1] at the end of the 18th century on mixtures of PC with a solid reducing phase (sugar or sulfur). Despite interesting energetic characteristics, no applications were found for these explosives because of their very high thermal and mechanical sensitivities. A lot of studies have been performed in order to desensitize the chlorate-based explosives, for instance by enrobing the chlorate particles by a viscous reducing liquid [2]. This led to the industrial development of compositions called “cheddites,” which were widely used in Europe at the beginning of the 20th century. Since then, the compositions containing chlorate were replaced by ammonium nitrate fuel oxidizer compositions (ANFO), which are cheaper, more powerful, and far less sensitive.

As a rule, the thermal decomposition of chlorate-based compositions is initiated by the decomposition of the reducing phase. For instance, this mechanism is observed in saccharose (Sa)- and thiourea-based compositions [3, 4]. Conversely, the decomposition is initiated by the melting of the chlorate when the reducing agent is thermally stable. Therefore, the thermal insensitivity of the reducing phase is the key point to desensitize a chlorate-based composition. Moreover, to obtain interesting energetic performances, the reducing agent must have a high density and be able to be mixed homogeneously with chlorate.

\* Corresponding author; e-mail: comet@isl.tm.fr

The idea developed at the ISL is to use nano-structured diamond as the reducing agent. This material has a high density, a good thermal stability in an oxidizing atmosphere and an energetic potential in principle higher than that of graphite. The nanostructuring favors mass transfer with chlorate. Nano-sized diamond was obtained by using a well known synthesis process [5, 6] and a purification treatment developed at the ISL [7]. The synthesis process consists in detonating an explosive mixture containing hexogen (RDX) and 2,4,6-trinitrotoluene (TNT) with respective weight percentages of 30 and 70%. The detonation soot is purified by filtrations followed by acidic and oxidation treatments.

The oxidizing phase used in this study is PC ( $\text{KClO}_3$ ), which exhibits excellent redox properties in the solid phase. Moreover, this salt is not very hygroscopic and has a high melting point (m.p. =  $356^\circ\text{C}$ ).

The energetic characteristics of nD- and PC-based compositions (noted nD/PC) were compared to those of the classical sugar and PC composition (denoted Sa/PC). These comparisons were performed by classical analysis methods. Thermal sensitivity was studied by differential scanning calorimetry (DSC). A fall hammer apparatus and a BAM friction test device were used to evaluate the impact and the friction sensitivity. The combustion of nD-based compositions was further characterized by time resolved cinematography (TRC) [8, 9]. The deflagration velocity was measured on the most interesting nD/PC energetic composition.

## 2 Experimental Part

### 2.1 Structural Characterization of Nanodiamonds, Potassium Chlorate, and Saccharose

The nDs were synthesized by detonation and then purified by a process developed at ISL. This process will not be detailed in this study.

Elementary analysis reveals that carbon, oxygen, nitrogen, and hydrogen are the main elements found in the nDs dried at  $150^\circ\text{C}$  (Table 1). The heteroatomic species (O, N, and H) belong to chemical functions surrounding the surface of the nD particles. They are mainly involved in the adsorption process of water from atmospheric moisture. The adsorbed water content ranges from 2 to 4% by weight. The total oxidation of the nDs performed by thermogravimetric analysis ( $\text{Ar}/\text{O}_2 = 80:20$ ) shows that the mineral ash content is around 3.6%. Energy dispersion spectrometry (EDS) reveals that these impurities are composed of iron, titanium, and silicon oxides. These phases come from the

synthesis process and cannot be totally removed by the purification treatment [7].

Transmission electron microscopy (TEM) pictures show that the nD particles have a 5 nm mean diameter (Figure 1A). The X-ray diffraction (XRD) pattern (Figure 1B) allows identification of the crystalline phases present in the sample. The figure is dominated by the (111) diffraction of diamond at  $44^\circ$  (JCPDS file 03-065-6329). Titanium dioxide ( $\text{TiO}_2$ ) and silica ( $\text{SiO}_2$ ) are also detected in the samples. The mean size of the nD crystallites can be calculated from the

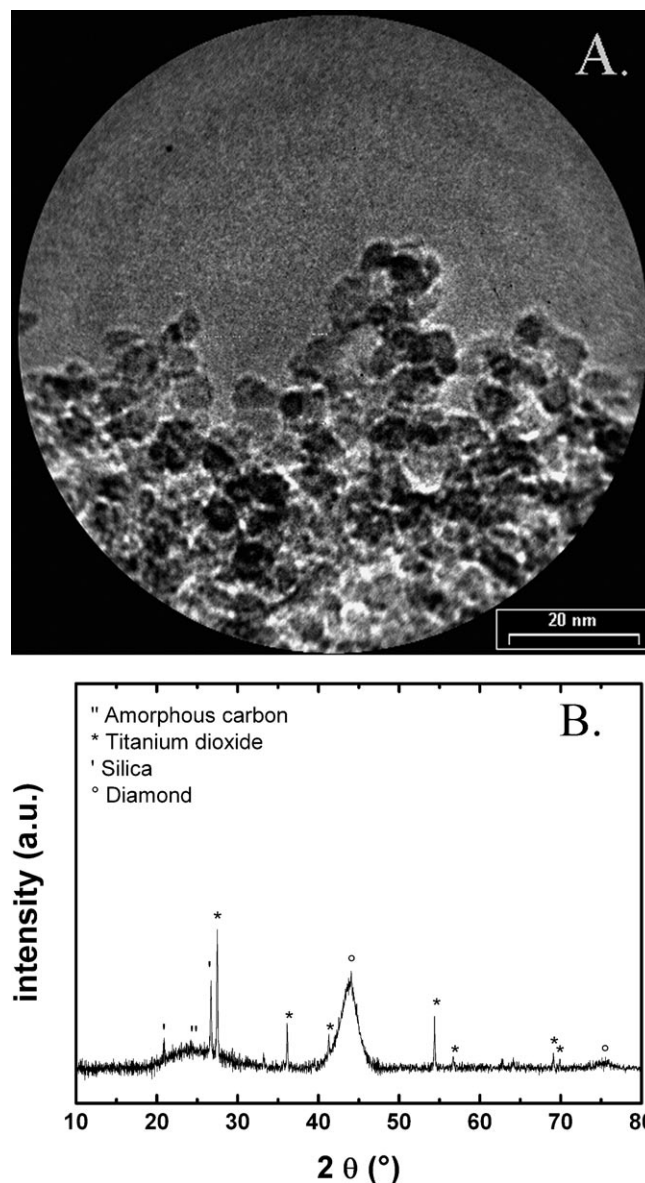


Figure 1. TEM picture (A) and XRD pattern (B) of nD.

Table 1. Chemical composition of the nD sample used to elaborate the nD/PC compositions.

Elements	C	O	H	N	S	Mineral ash Ti, Si, Fe, O
Mass Percentage (%)	80.42	12.82	0.74	2.42	<0.30	3.6

full-width at half maximum (FWHM) of the (111) diffraction peak of diamond ( $\text{FWHM} = 2.303^\circ$ ) by using the Scherrer equation. It was found to be 4.1 nm. The size of the elementary crystalline domains approximately corresponds to the size of individual particles observed by TEM.

The specific area of the nDs ( $S_{\text{BET/nD}} = 373 \text{ m}^2 \text{ g}^{-1}$ ) was measured by nitrogen adsorption by using the Brunauer–Emmett–Teller (BET) method. The sample had been outgassed at  $150^\circ\text{C}$  under vacuum. The mean diameter of the nDs ( $\Phi = 5.05 \text{ nm}$ ) can be calculated from the specific area value by assuming that the nDs are non-porous spherical particles [10]. The density ( $\rho_{\text{nD}} = 3.18 \text{ g cm}^{-3}$ ) was determined by helium pycnometry. This value is of course lower than the bulk density of diamond ( $\rho_{\text{D}} = 3.51 \text{ g cm}^{-3}$ ) because the surface functions contribute to a lower global density [7].

The PC (Prolabo, purity > 99%) and the Sa (Erstein) were ground in a mortar and then sifted using a  $50 \mu\text{m}$  sieve. To avoid caking by atmospheric moisture, these materials were stored in a desiccator containing phosphorus pentoxide. The particle size distribution was determined by laser granulometry after dispersion in isopropyl alcohol (Figure 2). It ranges from 1 to  $30 \mu\text{m}$  and from 2 to  $60 \mu\text{m}$  for the Sa and the PC particles, respectively. The density of the PC and the Sa was found to be equal to 2.33 and  $1.59 \text{ g cm}^{-3}$ , respectively.

## 2.2 Preparation Process of the Energetic Compositions

The energetic compositions were prepared by physical mixing of nD or Sa powders with PC. The proportions were defined to obtain compositions with a satisfying reactivity

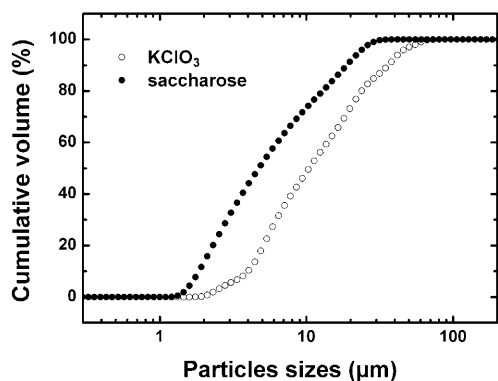


**Figure 2.** Particle size distribution of PC and Sa.

and a regular distribution on the formulation range (Table 2).

From an experimental point of view, the PC and the nDs (resp. Sa) were dispersed in 50 mL of petroleum ether to obtain 1–2 g of the final energetic composition. Petroleum ether was chosen as a dispersant because it dissolves none of the three solid phases. In addition, it is easily evaporated and hydrophobic, which limits the caking phenomenon induced by atmospheric moisture. In order to separate the particles, the suspension is magnetically stirred for 15 min and homogenized with an ultrasonic bath at the same time. Finally, the petroleum ether is extracted at  $60^\circ\text{C}$  under reduced pressure with a rotary evaporator. In order to avoid any mechanical stress, the composition adhering to the inner surface of the round-bottom flask was collected with a brush.

## 2.3 Structural Characterization of the Energetic Compositions

The specific area of the nD/PC compositions was measured by nitrogen adsorption using the well known BET equation. The adsorbed water was removed by a preliminary outgassing treatment ( $150^\circ\text{C}$ , vacuum, 45 min). The measured specific area ( $S_{\text{BET/meas}}$ ) corresponds to the weight balanced sum ( $\chi_{\text{PC}}; \chi_{\text{nD}}$ ) [11] of the specific areas of PC ( $S_{\text{BET/PC}}$ ) and nD ( $S_{\text{BET/nD}}$ ):

$$S_{\text{BET/meas}} = \chi_{\text{PC}} S_{\text{BET/PC}} + \chi_{\text{nD}} S_{\text{BET/nD}}$$

This result demonstrates that there is no interaction between the two components. The presence of a superficial water layer at the nD surface (0.1 nm thickness) could lead to an embedding of the nD particles by PC. This phenomenon would occur by a dissolution/crystallization cycle in the presence of atmospheric moisture. If this “in situ” PC nanostructuring phenomenon took place, the nD/PC compositions would have a specific area far more important than the one experimentally measured.

## 2.4 Reactive Characterization Methods

The DSC experiments were performed with a DSC Q1000 device (TA Instruments). Sealed crucibles purchased from the Institut Suisse de Sécurité were useful to perform the experiments under pressure. As the decomposition takes place in a confined volume, the complete energy released by

**Table 2.** Mass percentages of each composition according to the OB versus carbon dioxide.

nD-Based Compositions						
OB vs. $\text{CO}_2$	– 75.3	– 45.2	– 30.1	– 15.1	0	+ 15.1
nD/PC (%)	47.5: 52.5	34.9: 65.1	28.1: 71.9	22.0: 78.0	15.9: 84.1	10.2: 89.8
Sa-Based Compositions						
OB vs. $\text{CO}_2$	– 52.8	– 33.8	– 23.1	– 11.6	0.0	+ 14.6
Sa/PC (%)	60.7: 39.3	48.2: 51.8	41.1: 58.9	33.5: 66.5	25.9: 74.1	16.2: 83.8

the reaction could be measured. Two milligrams of each sample were used for each experiment.

The impact sensitivities were measured on  $40 \text{ mm}^3$  of powdered samples placed in steel cells with a diameter of 10 mm. The apparatus is equipped with a drop hammer (1 or 5 kg) which can fall down from an adjustable height of at most 1 m. A given test is considered as negative when no audible explosion occurs or when the content of the cell does not show pyrotechnic decomposition.

A Julius–Peters (BAM friction test) measuring device was used to determine the sensitivity of the materials to friction. The material laying down on a rough ceramic experiences friction from a ceramic stick. The force exerted by the stick (expressed in Newtons) is determined by the relative position of weights suspended by a lever. A test is assumed to be positive if a crackle, inflammation or change of color of the sample is observed. The impact (respectively friction) sensitivity threshold is defined as the minimal stress necessary to induce at least one pyrotechnic reaction among six tests.

The study of the combustion was performed by TRC [8, 9], an advanced method specifically devoted to the reactive characterization of energetic materials. Experimentally, the pelletized energetic material is ignited by a  $\text{CO}_2$  laser beam. Its output power is measured with a calorimeter and was found to be equal to 9 W. This power was delivered on a 4 mm diameter circular surface.

Two experimental values can be measured by this method: the ignition delay time (IDT) and the combustion speed. The IDT is the duration between the impact of the laser on the energetic material and the beginning of its combustion. It can be correlated to the density of surface energy necessary to initiate the material. The combustion velocity ( $V_c$ ) is measured by ultrafast cinematography using a Photron camera which is used at  $4000 \text{ frames s}^{-1}$  but can record up to  $125000 \text{ frames s}^{-1}$ . The camera is placed perpendicularly to the propagating combustion. For TRC characterization, the nD/PC powders have to be pelletized by pressing. The compression is performed on 50 mg samples with a hydraulic press which allows obtaining pressures from 12.3 to 557 MPa.

The deflagration velocity was measured in a brass cylindrical tube (Figure 3a) of 5 mm diameter, filled upto 80 mm of the total composition. The movement of the combustion front was measured by using three ionization probes regularly spaced at every 20 mm. The first probe is placed at 20 mm from the top of a PETN-based blasting cap. In the first 10 mm of the tube toward the probe no. 1, a larger hole (7 mm) was drilled in order to place the top of the detonator in contact with the nD/PC composition. The ionization probes are metallic needles insulated from the grounded cylinder (Figure 3b). When the deflagration occurs, thermal ionization induces an electrical short-cut between the needles and the cylinder. The time between the consecutive short-cuts allows the evaluation of the deflagration velocity of the charge. The nD/PC composition is compressed in successive steps between piston rods of

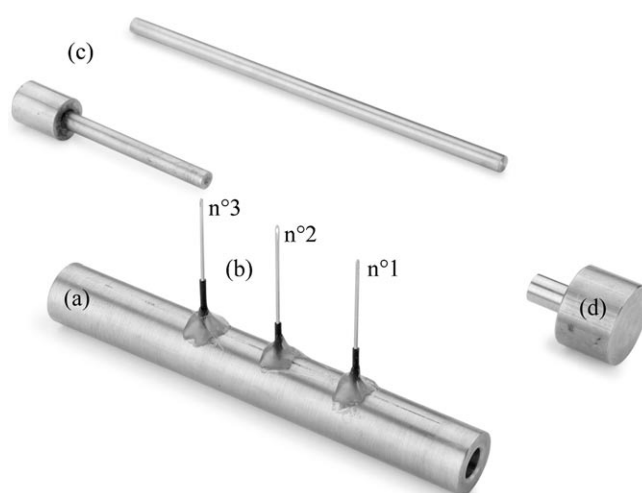


**Figure 3.** Device used to measure the deflagration velocity of the nD/PC compositions: the cylinder containing the energetic material (a), the ionization probes (b), the piston rods (c), and the removable metallic base (d).

different lengths (Figure 3c) and a removable metallic base (Figure 3d).

### 3 Results and Discussion

#### 3.1 Study of the Energetic Properties of Sa/PC and nD/PC Compositions

DSC was used to measure the energy released by the Sa/PC and nD/PC mixtures according to their oxygen balance (OB) versus carbon dioxide. The amounts of energy are calculated by integrating the decomposition exotherms. The decomposition temperature ( $T_{\text{dec}}$ ) reported here corresponds to the temperature at which the exotherm exhibits the maximum amplitude at a  $4 \text{ K min}^{-1}$  heating rate. The  $T_{\text{dec}}$  evolution gives a good indication of the relative thermal sensitivity of the mixtures Sa/PC and nD/PC.

The combustion of Sa-based mixtures provides a lot of energy. The maximum energy release is observed for the equilibrated OB ( $E_{\text{OB}=0} = 4.5 \text{ kJ g}^{-1}$ , Figure 4A). The amount of energy strongly depends on the Sa content as it is 2.6 times higher when the OB increases from  $-52.8$  to  $0\%$ . The most energetic composition is the most thermally sensitive as its decomposition temperature is the lowest ( $T_{\text{dec/OB}=0} = 154 \text{ }^\circ\text{C}$ ). The high thermal sensitivity of Sa/PC mixtures can be correlated to the thermal properties of Sa. Indeed, Sa melts at  $184 \text{ }^\circ\text{C}$  and then loses its hydroxyl groups at  $208 \text{ }^\circ\text{C}$ . PC contributes to lower the temperature of this chemical dehydration and acts as an activator for the combustion.

The maximum energy released by the combustion of the nD/PC compositions is reached for a negative OB ( $E_{\text{OB}=-30} = 3.4 \text{ kJ g}^{-1}$ , Figure 4B) and is lower than the maximum energy released by the combustion of the Sa/PC compositions. However, it can be noticed that the decom-

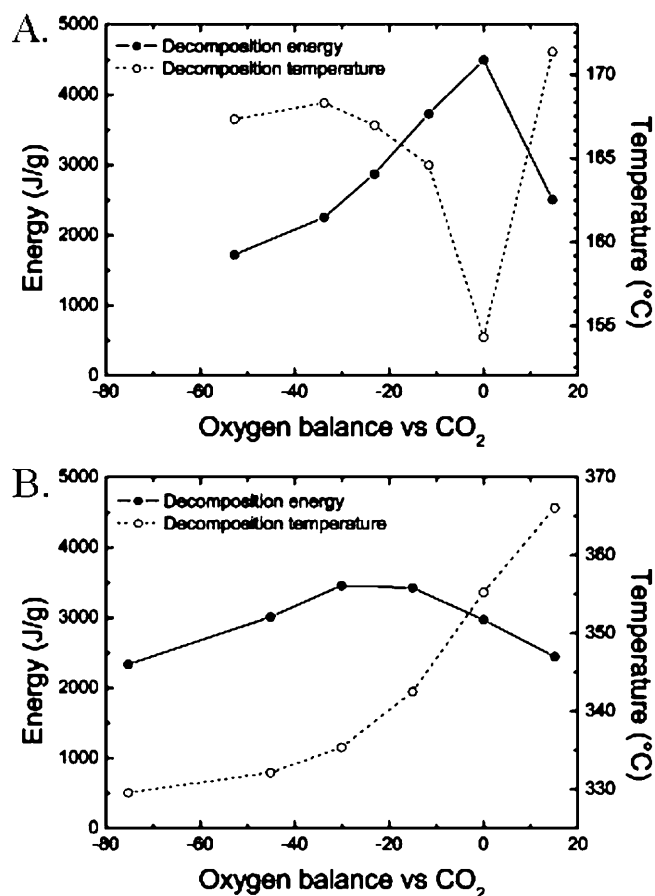


**Figure 4.** Energy and temperature of decomposition versus OB for Sa/PC (A) and nD/PC (B) compositions.

position energy is less dependent on the amount of reducing agent in the case of nD/PC compositions. From a thermal point of view, the nD/PC compositions are far less sensitive than their Sa/PC counterparts because their decomposition temperatures are above 330 °C. The chlorate-rich mixtures are the least sensitive. To understand the interaction mechanism between the nDs and the PC, these compounds were separately characterized by thermogravimetric analysis. Under a nitrogen atmosphere, the nDs are stable until 400 °C, whereas the PC melts at 356 °C. It can therefore be assumed that the combustion of nD/PC compositions is initiated by the oxidation of the nD surface functions by the PC and then the combustion self-propagates in the crystalline core of the nD particles. The excellent thermal conductivity of diamond (25 W cm<sup>-1</sup> K<sup>-1</sup> at 300 K [12]) allows a homogeneous diffusion of the combustion energy in the material. This is why the diamond-rich compositions exhibit low ignition temperatures.

### 3.2 Study of Sensitivity to Mechanical Stress

The impact sensitivity of nD/PC and Sa/PC compositions was studied depending on their OB (Figure 5A). The Sa-based compositions are generally more sensitive than the

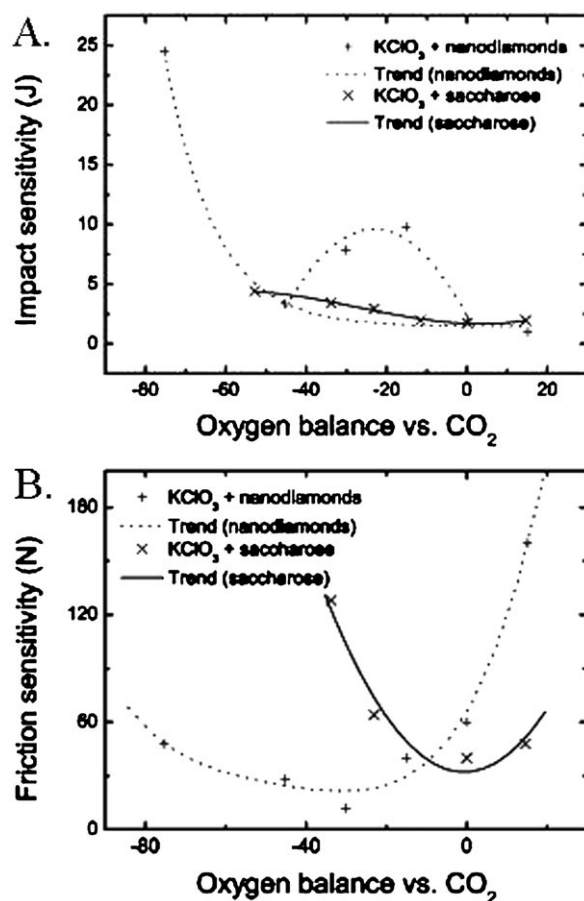


**Figure 5.** Evolution of the impact (A) and friction (B) sensitivity of nD/PC and Sa/PC mixtures with their OB.

ones containing nDs. The sensitivity threshold of Sa/PC compositions seems to be quite independent from the composition as it is between 1.74 and 4.4 J. The highest sensitivity is observed for an equilibrated OB. This result is in good agreement with the thermal analysis, which showed that the most energetic and the most thermally sensitive material had an equilibrated OB (Figure 4A). In contrast, the sensitivity threshold of nD/PC compositions ranges between 0.98 and 24.50 J (Figure 5A) and is very much dependent on the OB. When the nD content increases (negative OB), the compositions become less sensitive. The heat produced by the hammer impact on the sample is diffused in the bulk sample by the diamond because of its high thermal conductivity. In other words, the diamond acts as a desensitizing agent toward this kind of mechanical stress. Surprisingly, a substantial increase in the impact sensitivity threshold is observed for an OB equal to -30 and -15%. This result seems to be particularly interesting because these two compositions are among the more energetic (Figure 4B).

The appearance of the friction sensitivity threshold for nD/PC compositions is more classical as it reaches its minimum for the most energetic sample (12 N, OB = -30%, Figure 5B). An excess of nD or PC desensitizes the compositions. However, nD-rich nD/PC compositions

are much more sensitive to friction than Sa-rich Sa/PC compositions. This behavior is easy to understand insofar as the diamond is the hardest mineral phase. So, a friction stress results in a scratching of the surface of the chlorate particles by the nDs.

Concerning the Sa/PC compositions, the highest sensitivity is observed for an equilibrated OB (40 N, OB = 0%), which corroborates the DSC and hammer-fall results.

### 3.3 Molding of Energetic Compositions

The characterization of nD/PC compositions by TRC requires molding the powders by compression in order to obtain pelletized materials (Figure 6B). The nD/PC and Sa/PC compositions are sufficiently insensitive to pressure. The mold used to press the compositions was a steel cylindrical device (Figure 6A).

It had a 4 mm diameter and 30 mm length. In order to get enough material and to limit the friction stress when the pellet is pulled out, the pressed amounts must not exceed 50 mg. The pressing was studied by calculating the compaction ratio (CR) according to the composition and pressure. The latter depends on the load on the lever arm of the hydraulic press. The CR is obtained by dividing the apparent density of a pellet by its theoretical maximum density (TMD). The apparent density ( $\rho_{ap}$ ) is calculated from the weight ( $m_{pel}$ ), the diameter ( $\Phi_{pel}$ ), and the height ( $h_{pel}$ ) of the pellet. The TMD corresponds to the weighted sum (volume fractions  $\chi_{PC}$  and  $\chi_{nD}$ ) of the densities of PC and nD ( $\rho_{PC}$ ,  $\rho_{nD}$ , respectively):

$$CR = 100 \times \frac{\rho_{ap}}{TMD} = \frac{400m_{pel}}{\pi\Phi_{pel}^2 h_{pel} (\chi_{PC}\rho_{PC} + \chi_{nD}\rho_{nD})}$$

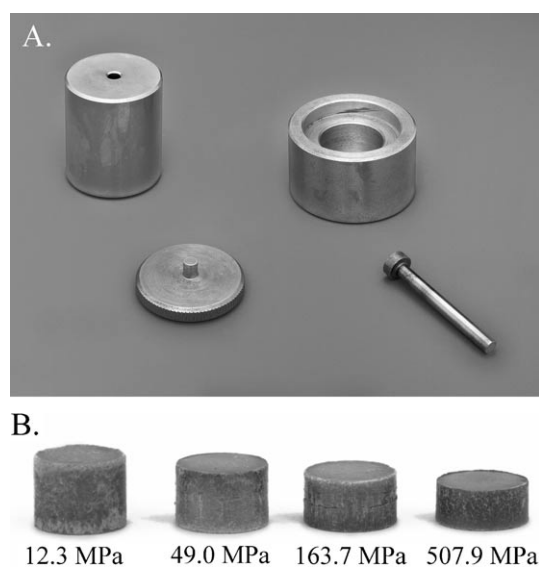


**Figure 6.** Mold used to press the nD/PC and Sa/PC compositions (A), nD/PC pellets (34.9% nD) obtained for different pressing levels (B).

The CR logically increases with the pressure (Figure 7a). The more compressible materials exhibit a CR slightly higher than 90%. This value corresponds to the ideal space filling by a bimodal particle size distribution. For a close packing of particles similar to the ones used in crystallography (such as fcc or hcp) [13], it can be assumed that the biggest particles (here, PC particles) fill 74% of the total volume. The nDs, which are the smallest particles, fill 74% of the remaining space between the PC particles. This allows the calculation of a theoretical limit CR ( $CR_{lim.}$ ):

$$CR_{lim.} = 74 + \frac{(100 - 74) \times 74}{100} \approx 93.2\%$$

This  $CR_{lim.}$  can be reached for an nD volume content smaller than 19.2% (24.5% by weight). When the nD/PC compositions contain a lot of nD, the CR calculated from experimental regression equations for an infinite pressure tends to 80%. In other words, the more a composition contains nanosized particles, the harder it is to get a high CR. This is a logical result as the resistance to pressing depends on the external surface of the particles. A nD-rich composition is more difficult to compress as its specific area is higher. The presence of a nanostructured phase in an energetic composition requires the use of a very high pressure to improve the density. The surface interactions are tremendously improved by nano-structuring, and the excep-

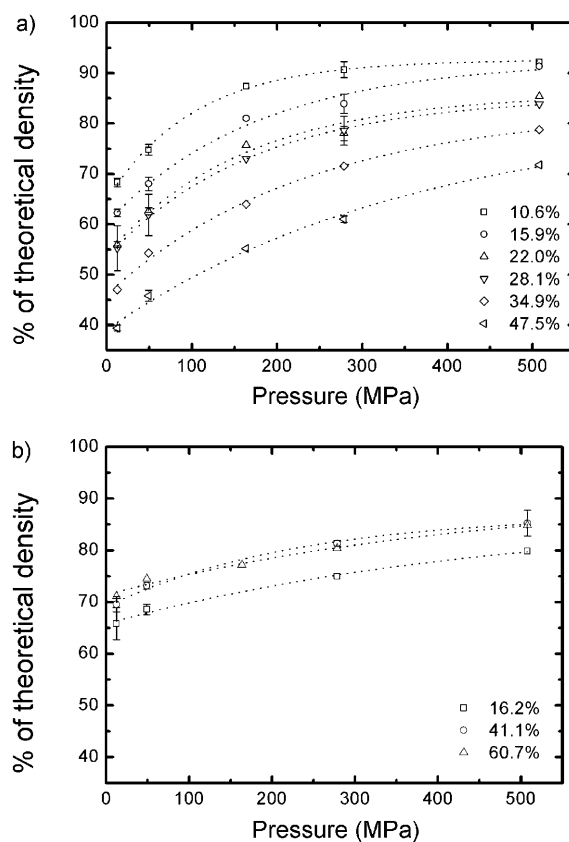


**Figure 7.** Variation of the compaction rate according to the pressure for different nD (a) and Sa (b) contents.

tional cohesion of nD/PC compositions (Figure 6B) can be assigned to these effects. For instance, even the pellets having a CR lower than 40% are cohesive and can be easily manipulated. The Sa/PC compositions (Figure 7B) with a high chlorate content are more difficult to compress than the compositions containing larger amounts of Sa. As the Sa and PC particles have sizes of the same order of magnitude, the space filling can be attributed to the crushing of Sa particles. For the micron-sized Sa/PC mixtures, the compaction rate variation is less important than for nD/PC mixtures.

### 3.4 Study of the Combustion of nD/PC Pellets by Time-resolved Cinematography

nD/PC pellets were ignited by a laser beam to characterize their combustion by TRC. The laser used delivers a 9 W power on a 12.6 mm<sup>2</sup> surface.

Two decomposition mechanisms were observed. The first one corresponds to a continuous auto-propagated combustion in which the ignition front moves parallel to the laser beam. The second one is characterized by an intermittent combustion which gives periodical pulses (Table 3). The materials undergoing a pulsed combustion are less sensitive to thermal stress than the others, which is confirmed by the DSC results (Figure 4). The surface activation energy required to initiate the combustion of the pellets was calculated from the IDTs (Figure 8) and ranges from 2.9 to 21.6 J cm<sup>-2</sup>. The samples with a higher nD content exhibit shorter IDTs, i.e., they are more sensitive to thermal stress

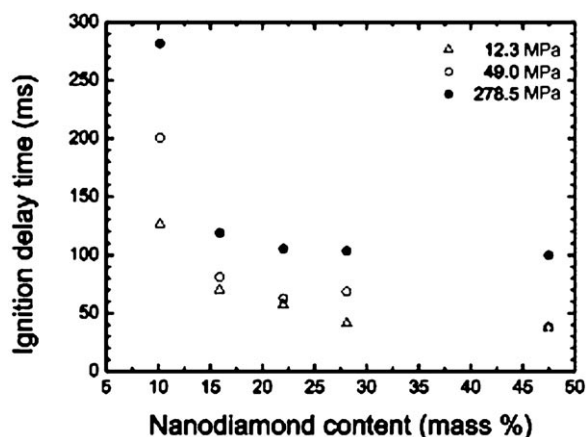


**Figure 8.** IDT of nD/PC represented as a function of the nD content and the pressure.

**Table 3.** Combustion mode and velocities of nD/PC compositions according to their compression conditions.

nD Content (w%)	12.3 MPa	49.0 MPa	278.5 MPa
10.2	Pulse	Pulse	Pulse
15.9	Pulse	Pulse	Pulse
22.0	$3.96 \pm 0.06$ cm s <sup>-1</sup>	$3.44 \pm 0.02$ cm s <sup>-1</sup>	Pulse
28.1	$2.15 \pm 0.10$ cm s <sup>-1</sup>	$2.05 \pm 0.19$ cm s <sup>-1</sup>	Pulse
47.5	$0.57 \pm 0.01$ cm s <sup>-1</sup>	$0.61 \pm 0.16$ cm s <sup>-1</sup>	$0.54 \pm 0.11$ cm s <sup>-1</sup>

(Figure 8). When the nD content is higher than 20%, the IDT is constant and depends only on the pressing level used for pelletization. Pressing strongly decreases the thermal sensitivity of nD/PC compositions.

The combustion velocities (Table 3) were measured on non-confined pellets having a continuous combustion. They are typical of a slow combustion as they range from 0.54 to 3.96 cm s<sup>-1</sup>. As a general rule, they decrease when the nD content and the pressing level increase.

### 3.5 Deflagration Velocity Measurement

The deflagration velocity was measured on a slightly under-oxygenated nD/PC mixture (OB = -30%). This composition was chosen because the thermal analysis revealed that it was the most energetic one (Figure 4B). As this material is friction-sensitive, it was pressed step by step: amounts of 0.20 g were successively compressed until the height of the mixture had reached 80 mm in the cylindrical device previously described (Figure 3). The compacting was performed with a hydraulic press giving a 12.6 MPa pressing level. This pressure provides a good cohesion to the material and allows to minimize experimental hazards. The loading density was 1.00 g cm<sup>-3</sup>, which represents only 47.3% of the TMD (TMD = 2.12 g cm<sup>-3</sup>).

Reported velocities in Table 4 correspond to the propagation of the deflagration front between the ionization probes, which are 20 mm away from each other. The recorded speeds are typical of a deflagration process. Visual observations of the tubes after firing confirm that no detonation occurred as long as the metal burst only took place along about 3 cm near the detonator. The part of the tube where the no. 2 and 3 ionization probes were localized remains intact. The mean velocity recorded between no. 1 and 2 probes is higher than the one measured between no. 2 and 3 probes. This result indicates that there is no transition from deflagration to detonation. Moreover, the deflagration process primed by a detonation (Table 4) is four orders of magnitude faster than the combustion propagation initiated by a laser beam in a non-confined environment (Table 3).

## 4 Conclusion

To our knowledge, nD particles were never used before as a reducing agent in energetic explosive compositions. The aim of this study was to demonstrate the feasibility and the efficiency of nD-based compositions. For this purpose,

**Table 4.** Duration of the deflagration propagation between the ionization probes ( $\delta t$ ) and the corresponding deflagration velocities ( $V$ ).

	Cylinder No. 1		Cylinder No. 2		Cylinder No. 3		Mean Nos. 1, 2, 3 ( $V$ ) (m s <sup>-1</sup> )
	$\delta t$ ( $\mu$ s)	$V$ (m s <sup>-1</sup> )	$\delta t$ ( $\mu$ s)	$V$ (m s <sup>-1</sup> )	$\delta t$ ( $\mu$ s)	$V$ (m s <sup>-1</sup> )	
Probe No. 1 $\rightarrow$ 2	16.55	1208	16.20	1234	17.60	1136	1193 $\pm$ 51
Probe No. 2 $\rightarrow$ 3	25.74	777	22.00	909	24.00	833	840 $\pm$ 66

mixtures of nD (5 nm in diameter) and PC (nD/PC) were investigated and compared to the well known Sa and PC (Sa/PC) compositions.

The nD/PC compositions are far less sensitive to thermal stress than the classical Sa/PC compositions. The Sa content in Sa/PC mixtures seems to have little effect on their impact sensitivity. This is not the case for nD/PC compositions; their impact sensitivity strongly depends on the nD content. It was found that the nD/PC compositions exhibit a high sensitivity to friction due to the hardness of the diamond. However, chlorate-rich nD/PC compositions are quite insensitive to friction stress.

The nD/PC powders can be molded by compression. The resulting pellets have an impressive mechanical cohesion, even for CRs as low as 40% of the TMD. However, it can be stressed that the presence of nD particles requires very high pressures to make the nD/PC powders dense.

The nD/PC compositions are deflagrating primary explosives. They are dense, not sensitive to thermal stress, stable, and nontoxic. These explosives can be considered as "green" primers as they contain neither heavy metals (lead, quicksilver) nor phosphorus. Additionally, their decomposition products are nonhazardous: potassium chloride, carbon dioxide, and water.

Further studies on the aging of nD/PC compositions will soon be performed. The effect of the PC nanostructure on the reactivity of nD/PC compositions will be assessed. The energetic properties of potassium perchlorate- and nD-based compositions will also be evaluated to obtain less sensitive and denser explosive mixtures.

## 5 References

- [1] M. Comet, H. Fuzellier, Etude Synoptique des Explosifs, *L'Act. Chim.* **2000**, 7–8, 4.
- [2] H. Kast, *Spreng- und Zündstoffe*, Vieweg & Sohn, Braunschweig **1921**, 344–373.
- [3] R. K. Barton, A. J. Barratt, Observations on the Reactivity of Pyrotechnic Compositions Containing Potassium Chlorate and Thiourea, *Propellants, Explos., Pyrotech.* **1993**, 18, 77.
- [4] M. Comet, L. Schreyeck, H. Fuzellier, An Efficient Composition for Bengal Lights, *J. Chem. Educ.* **2002**, 79, 70.
- [5] V. M. Titov, V. F. Anisichkin, I. Y. Mal'kov, Synthesis of Ultrafine Diamonds in Detonation Waves, *9th Symposium (International) on Detonation*, Portland, Oregon, USA, August 28–September 1, **1989**, p. 407.
- [6] E. Fousson, *Formation de Diamants par Voies Dynamiques et Leur Caractérisation*, Thèse de l'Université de Haute Alsace, Mulhouse, France **2000**.
- [7] V. Pichot, M. Comet, E. Fousson, C. Baras, A. Senger, F. Le Normand, D. Spitzer, An Efficient Purification Method for Detonation Nanodiamonds, Carbon, *Diamond Relat. Mater.* **2008**, 17, 13.
- [8] J. J. Granier, M. L. Pantoya, Laser Ignition of Nanocomposite Thermites, *Combust. Flame* **2004**, 138, 373.
- [9] M. Comet, D. Spitzer, Elaboration and Characterization of Nano-sized AlxMoyOz/Al Thermites, *33rd International Pyrotechnics Seminar*, Fort Collins, Colorado, USA, July 16–21 **2006**, p. 93.
- [10] G. Xiong, Z. Zhi, X. Yang, L. Lu, X. Wang, Characterization of Perovskite-Type LaCoO<sub>3</sub> Nanocrystals Prepared by a Stearic Acid Sol-Gel Process, *J. Mater. Sci. Lett.* **1997**, 16, 1064.
- [11] D. Spitzer, M. Comet, J.-P. Moeglin, E. Stechele, U. Werner, Y. Suma, Synthesis and Investigation of the Reactivity of Nano Thermite Mixture, *37th International Annual Conference of ICT*, Karlsruhe, June 27–30 **2006**, p. 117/1.
- [12] T. Gehin, *Mise en œuvre de l'Épitaxie par Jets Moléculaires pour la Synthèse de Diamant Monocristallin*, Thèse de l'Université des Sciences et Technologies de Lille, Lille, France **2004**.
- [13] A. Casalot, A. Durupt, *Chimie Inorganique*, Hachette, Paris **1993**, p. 49.

## Acknowledgements

The authors would like to thank Alain Boffy and Yves Suma who contributed to time resolved cinematography measurements. They are grateful to Auguste Ritter and Jean-Marie Brodbeck who conceived the experimental device that was used to measure the deflagration velocity.

## Symbols and Abbreviations

$\rho$	Density (g cm <sup>-3</sup> )
$\chi$	Weight ratio (%)
$\Phi$	Particles diameter (nm)
CR	Compaction ratio
DSC	Differential scanning calorimetry
nD	Nanodiamond
OB	Oxygen balance (%)
PC	Potassium chlorate
Sa	Saccharose
$S_{\text{BET}}$	Specific area calculated from Brunauer–Emmett–Teller equation (m <sup>2</sup> g <sup>-1</sup> )
TEM	Transmission electron microscopy
TMD	Theoretical maximal density
TRC	Time resolved cinematography
XRD	X-ray diffraction